

# Organelle-specific, rapid induction of molecular activities and membrane tethering

Toru Komatsu<sup>1,3</sup>, Igor Kukelyansky<sup>1,3</sup>,  
J Michael McCaffery<sup>2</sup>, Tasuku Ueno<sup>1</sup>,  
Lidenys C Varela<sup>1</sup> & Takanari Inoue<sup>1</sup>

**Using new chemically inducible dimerization probes, we generated a system to rapidly target proteins to individual intracellular organelles. Using this system, we activated Ras GTPase at distinct intracellular locations and induced tethering of membranes from two organelles, endoplasmic reticulum and mitochondria. Innovative techniques to rapidly perturb molecular activities and organelle-organelle communications at precise locations and timing will provide powerful strategies to dissect spatiotemporally complex biological processes.**

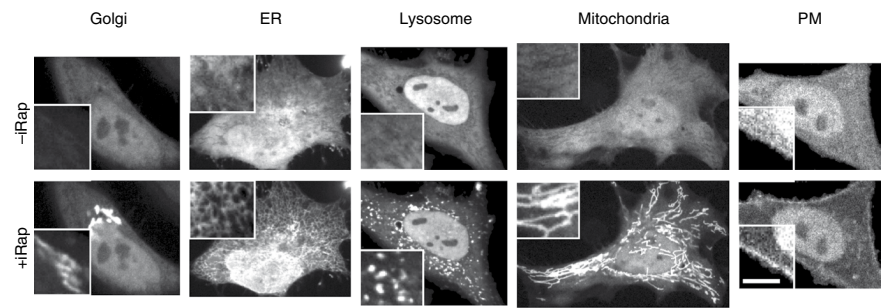
Signaling events in many cells are local and rapid, and they can compensate for certain cell perturbations. Therefore, elucidating the structure and function of complex signaling networks requires perturbation that is faster than the signaling events themselves, that acts in precisely defined spatial domains and that can be applied at desired time points. Based on a rapamycin-driven heterodimerization technique<sup>1</sup>, we have previously introduced chemical-molecular tools that allow inducible, quick-onset and specific perturbation of various signaling molecules in living cells<sup>2,3</sup>. However, the use of these tools is restricted to proteins that are active at the plasma membrane<sup>2,3</sup> or in endosomes<sup>4</sup>. Considering that most signaling events are regulated in concert at multiple intracellular locations, we have begun to develop

perturbation strategies that can be used at Golgi, mitochondria, endoplasmic reticulum (ER) or lysosomes. Here we demonstrate how the heterodimerization technique can be used to recruit a protein of interest to any one particular organelle.

In this system, one of the dimerization partners, FKBP binding protein (FKBP) or FKBP-rapamycin binding domain (FRB), is anchored to the cytoplasmic face of the organelle (anchor unit) and the other is left available within the cytoplasm as a fusion with protein of interest (effector unit). Addition of chemical dimerizers such as rapamycin or its analogs (for example, indole rapamycin<sup>2</sup> (iRap)) induces translocation of the protein of interest to the surface of the organelle through the formation of the FKBP-FRB complex. To develop anchor units for Golgi, we tested several Golgi targeting motifs by fusing them to FKBP or FRB. A Golgi-targeting motif from giantin localized properly and did not alter the Golgi structure upon overexpression (Supplementary Fig. 1a). Using general morphology as a cytotoxicity index, we selected minimally disruptive targeting motifs for other organelles (Supplementary Fig. 1b and Supplementary Table 1). We assured their specificity by expressing these anchor units together with orthogonal organelle markers (Supplementary Fig. 2). Then, we expressed a cytoplasmic dimerization partner consisting of FKBP or FRB labeled with a fluorescent protein along with one of the anchor units. Upon iRap addition, the effector unit within seconds translocated from the cytoplasm to the site of the anchor unit. After optimizing protein configuration (Online Methods), we transfected the following anchor and effector units: FRB-YFP-Giantin and CFP-FKBP for Golgi; FRB-MoA and CFP-FKBP for mitochondria; CFP-FKBP-Cb5 and YFP-FRB for ER; LAMP-CFP-FRB and YFP-FKBP for lysosome; and Lyn-FRB and CFP-FKBP<sup>2</sup> for the plasma membrane (Fig. 1, Supplementary Videos 1–4 and Supplementary Fig. 3).

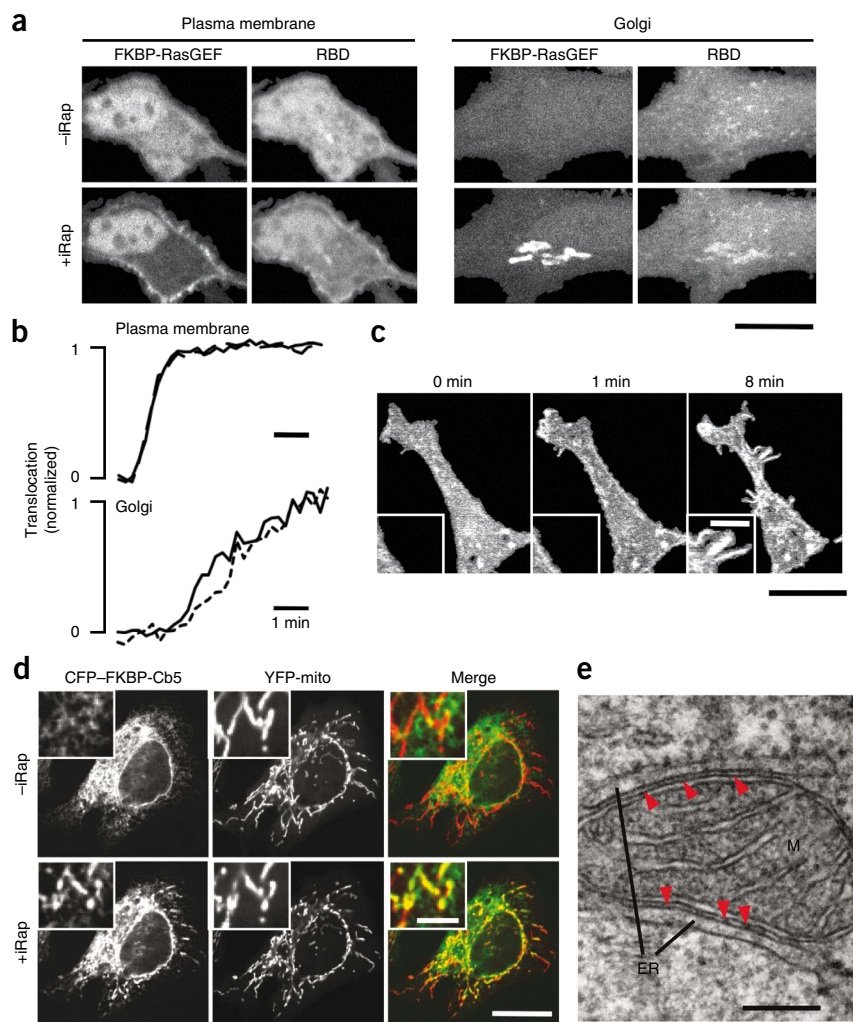
The FRB protein used in the study has a mutation (T2098L) that makes the protein unstable by itself but stable in the presence of chemical dimerizers and FKBP<sup>5</sup>. We therefore quantified expression of FRB fusion proteins with or without iRap and their FKBP partners. Based on a western blot analysis, we observed

**Figure 1** | Chemically inducible recruitment of cytoplasmic proteins to various organelles. Confocal fluorescence images of HeLa cells expressing FRB-YFP-Giantin and CFP-FKBP for Golgi, FRB-MoA and CFP-FKBP for mitochondria, CFP-FKBP-Cb5 and YFP-FRB for ER, and LAMP-CFP-FRB and YFP-FKBP for lysosome imaged before and after addition of 5  $\mu$ M iRap for 5 min, which induced translocation of the constructs. Representative images of 12, 13, 22 and 9 cells examined for Golgi, mitochondria, ER and lysosome, respectively. Scale bars, 20  $\mu$ m (insets, 5  $\mu$ m).



<sup>1</sup>Department of Cell Biology, Center for Cell Dynamics, School of Medicine and <sup>2</sup>Integrated Imaging Center, Department of Biology, Johns Hopkins University, Baltimore, Maryland, USA. <sup>3</sup>These authors contributed equally to this work. Correspondence should be addressed to T.I. (jctinoue@jhmi.edu).

**Figure 2** | Implementation of organelle recruiting system to probe the role of signaling molecules and interorganelle interactions. **(a)** Confocal fluorescence images of HeLa cells expressing FKBP-RasGEF, Lyn-FRB or FRB-Giantin, and YFP-labeled Ras biosensor (RBD), show the recruitment of a FKBP-RasGEF to the plasma membrane (left) or Golgi (right) upon iRap (5  $\mu$ M) addition for 5 min. **(b)** Analysis of RasGEF translocation (solid lines) and Ras activation (dotted lines). **(c)** Confocal fluorescence images of NIH3T3 cells expressing FKBP-RasGEF and Lyn-FRB. iRap was added after the 0 min image was collected and the other images were collected at indicated times after iRap addition. **(d)** Confocal fluorescence images of HeLa cells expressing CFP-FKBP-Cb5 (ER marker), Tom20-FRB and YFP-labeled mitochondrial marker (YFP-mito, middle) before and after addition of 5  $\mu$ M iRap for 5 min. Merged images show cyan (green, ER) and yellow (red, mitochondria) fluorescence. **(e)** TEM images of membrane junction sites created by inducible ER-mitochondria connection. HeLa cells expressing Tom20-YFP-FRB and CFP-FKBP-Cb5 were treated with 5  $\mu$ M iRap for 15 min and then processed for TEM. Arrowheads mark junction sites. M, mitochondria. Scale bars, 20  $\mu$ m (**a,c,d**), 5  $\mu$ m (insets in **c,d**) and 500 nm (**e**).



reasonable expression of Tom20-YFP-FRB and FRB-YFP-Giantin, which may be a consequence of a strong cytomegalovirus promoter and transient transfection. Moreover, Tom20-YFP-FRB expression was not affected by iRap treatment for 15 min, the time window relevant for the biological assays in the present study (**Supplementary Fig. 4**). This observation is consistent with the relatively slow kinetics reported for chemical dimerizer-induced stabilization of FRB proteins (a timescale of hours)<sup>5,6</sup>.

We sought to achieve precise spatiotemporal perturbation of signaling components in complex networks. First, we activated Ras small GTPases at different intracellular locations. Complexity in signaling networks is often derived from a few sets of proteins being co-opted for multiple tasks. Ras GTPases regulate not only cell proliferation and differentiation but also cell migration and T-cell activation. This diversity of function is thought to stem from the proteins' spatiotemporal compartmentalization<sup>7</sup>. For example, the activation of Ras' downstream effectors exhibits different activation kinetics (transient versus sustained) depending on whether cells undergo proliferation or differentiation<sup>8</sup>. Additionally, Ras activation has been observed at the plasma membrane and/or the Golgi in T cells depending on the type of stimulus<sup>7</sup>. To distinguish between Ras activation emanating from the plasma membrane of the Golgi, we expressed organelle-specific anchor units together with an effector unit consisting of a guanine nucleotide exchange factor for Ras (RasGEF). The use of RasGEF instead of engineered Ras alone to activate the Ras signaling pathway allows for more natural manipulation by activating 'endogenous' Ras. iRap addition induced a rapid translocation of the RasGEF to the plasma

membrane or Golgi, where we used Lyn-FRB<sup>2</sup> or FRB-giantin, respectively, as the anchor unit (**Fig. 2a**). Using a fluorescent biosensor for Ras, we visualized Ras activity and confirmed that Ras activation occurred strictly at each organelle (**Fig. 2a**). At the plasma membrane, both RasGEF translocation and Ras activation occurred rapidly (~1 min), but at Golgi, there was slower RasGEF translocation (~3 min) as well as slightly delayed Ras activation (**Fig. 2b**). The slower kinetics for the RasGEF recruitment to Golgi may be due to intricate membrane structures that limit access of bulky fusion proteins like RasGEF labeled with CFP and FKBP. Notably, the cells started to form membrane ruffles a few minutes after Ras activation at the plasma membrane (**Fig. 2c**). In contrast, Ras activation at Golgi did not result in any obvious change in cell morphology. This observation supports the compartmentalized role of Ras; active Ras at the plasma membrane, but not at Golgi, can regulate actin cytoskeleton. Alternatively, differences in the activation level of Ras at the plasma membrane or the Golgi may explain the observed phenotypes. Using immunohistochemistry, we visualized ERK phosphorylation, one of the major Ras downstream actions. Ras activation at the plasma membrane for 15 min induced ERK phosphorylation preferentially in the nucleus, which resembles the phenotype with EGF stimulation (**Supplementary Fig. 5a,b**). In contrast, upon Ras activation at the Golgi for 15 min, we detected phospho-ERK primarily at the Golgi

(Supplementary Fig. 5c). The spatially distinct ERK activation suggested that there was no cross-talk between the Ras pathways derived from the two different compartments in this time window.

Rapamycin and its analogs are known to inhibit mTOR activity, which may in turn affect other signaling pathways including the Ras-MAPK pathway, thus potentially limiting its use as a dimerizer. Given that a major role of mTOR is protein translation, which requires hours to take effect, a biological event that occurs with a timescale of seconds to minutes will not likely be affected by rapamycin-mediated mTOR inhibition. To test this, we quantified phospho-ERK induced by EGF stimulation in the presence or absence of rapamycin or iRap and found that 15 min of induction by iRap and EGF did not perturb ERK phosphorylation (Supplementary Fig. 6). There are some reports that rapamycin-driven dimerization system is reversible on the order of hours<sup>9</sup>. Our fusion constructs however did not show reversibility within 10 h. Nevertheless, selective activation of signaling molecules including Ras at various intracellular compartments will be a powerful means to delineate their short term spatiotemporal dynamics and functions.

Organelles are highly dynamic entities that interact with and disengage from one another. Through such physical contacts, they communicate and exchange information. Therefore, we developed a strategy to artificially tether intracellular membranes from two different organelles. An association between mitochondria and ER (now known as mitochondria-associated membranes, MAMs) has been first characterized by fluorescence imaging<sup>10</sup>. Subsequent work has suggested that this physical interaction places two organelles so close to each other that  $\text{Ca}^{2+}$  released from ER can be quickly taken up by juxtaposed mitochondria, which affects the propensity toward apoptosis<sup>11</sup>. Furthermore, multiple lipid enzymes have been identified at the MAMs, suggesting their role in lipid metabolism<sup>12</sup>. Most recently, Mitofusin 2 has been identified as a molecular entity that brings about the ER-mitochondria connection<sup>13</sup>. To rapidly reconstitute MAMs in living cells, we expressed the anchor units for both ER and mitochondria and induced heterodimerization to connect two membranes. The strategy was based on 'constitutive' tethering of ER to mitochondria using a chimaeric protein that has two targeting motifs<sup>14</sup>, as well as chemical dimerizer-mediated 'inducible' tethering of plasma membrane to ER<sup>15</sup> or to synaptic vesicles<sup>9</sup>. iRap addition to cells co-expressing two anchor units in the ER and mitochondria induced a striking morphological change; the typical meshwork-like structure of ER suddenly assumed a tubular shape that is more typical of mitochondria (Fig. 2d; we observed the tethering phenotype in 7 out of 10 cells). Simultaneous visualization of both organelles using confocal microscopy confirmed that the newly emerging tubular ER structure overlapped and traveled together with mitochondria (Supplementary Videos 5,6 and Supplementary Fig. 3). Conventional thin-section electron microscopy (TEM) analysis revealed that the two organelles were next to each other with  $6.6 \pm 1.4$  nm separations (Fig. 2e). We did not find conclusive evidence for membrane fusion under these conditions; but we observed well-delineated tethers spaced irregularly between the two organellar membranes (Supplementary Fig. 7a,b). Untransfected, untreated cells exhibited good separation between the two membranes ( $93.0 \pm 84.2$  nm; Supplementary Fig. 7c). We then synthetically induced MAMs and simultaneously visualized lipid molecules. Whereas fluorescent dye-labeled

phosphatidylserine (NBD-PS) was initially distributed to Golgi and mitochondria, NBD-PS accumulated at the junction sites upon induction of synthetic MAMs (Supplementary Fig. 8). Finer characterization will be required to distinguish whether the lipid was transferred to the ER membranes through the MAMs. We also tested other combinations of the anchor units and found that lysosomes can be tethered to ER as well as to mitochondria and that ER can be tethered to Golgi (Supplementary Fig. 9). ER was often the organelle that altered its shape and moved with respect to the others, suggesting an inherent plastic nature in its structure and dynamics in addition to its ubiquitous distribution in the cells.

This approach using chemically inducible dimerization probes should complement prevailing perturbation methods and offer additional information regarding spatiotemporal dynamics.

## METHODS

Methods and any associated references are available in the online version of the paper at <http://www.nature.com/naturemethods/>.

Note: Supplementary information is available on the Nature Methods website.

## ACKNOWLEDGMENTS

We thank B. Wattenberg (University of Louisville) for Cb5/MoA plasmids; N. Ishihara (Toyko Medical and Dental University) for Tom20 plasmid; C. Machamer (Johns Hopkins University) for Giantin plasmid; W.D. Heo (Korea Advanced Institute of Science and Technology) for RasGRF plasmid; F. Tsuruta (University of Tsukuba) for LAMP plasmid; M. Fivaz (Duke-National University of Singapore Graduate Medical School Singapore) YFP-RBD plasmid; and T. Wandless (Stanford University) for providing rapamycin analogs (iRap, synthetic ligand of FKBP, FK506M); F. Fernandez, M. Fivaz, M. Meffert, J. Zhang, V. Sample, D. Montell, M. Caterina, P. Devreotes, A. Ewald and D. Robinson for critical review of the manuscript; R. Pagano for helpful comments on PS assays; and Z. Wei, W. Wong, K. Venkatachalam and J. Cordon for a technical assistance with western blot analyses. Supported in part by US National Institutes of Health (MH084691 to T.I., NCRR1S10RR023454-01 to J.M.M.). T.K. and T.U. are recipients of a fellowship from Japanese Society for the Promotion of Science.

## AUTHOR CONTRIBUTIONS

T.K., I.K., T.U., L.C.V. and T.I. designed and conducted molecular/cellular biology experiments with following data analysis. J.M.M. took and analyzed TEM images. T.I. conceived and supervised the project, and wrote the paper.

## COMPETING INTERESTS STATEMENT

The authors declare no competing financial interests.

Published online at <http://www.nature.com/naturemethods/>.

Reprints and permissions information is available online at <http://npg.nature.com/reprintsandpermissions/>.

- Schreiber, S., Kapoor, T.M. & Wess, G. *Chemical Biology: From Small Molecules to Systems Biology and Drug Design* (Wiley-VCH, 2007).
- Inoue, T., Heo, W.D., Grimley, J.S., Wandless, T.J. & Meyer, T. *Nat. Methods* **2**, 415–418 (2005).
- Suh, B.C., Inoue, T., Meyer, T. & Hille, B. *Science* **314**, 1454–1457 (2006).
- Fili, N., Calleja, V., Woscholski, R., Parker, P.J. & Larijani, B. *Proc. Natl. Acad. Sci. USA* **103**, 15473–15478 (2006).
- Stankunas, K. et al. *ChemBioChem* **8**, 1162–1169 (2007).
- Stankunas, K. et al. *Mol. Cell* **12**, 1615–1624 (2003).
- Mor, A. & Philips, M.R. *Annu. Rev. Immunol.* **24**, 771–800 (2006).
- Marshall, C.J. *Cell* **80**, 179–185 (1995).
- Karpova, A.Y., Tervo, D.G., Gray, N.W. & Svoboda, K. *Neuron* **48**, 727–735 (2005).
- Soltys, B.J. & Gupta, R.S. *Biochem. Cell Biol.* **70**, 1174–1186 (1992).
- Pizzo, P. & Pozzan, T. *Trends Cell Biol.* **17**, 511–517 (2007).
- Hayashi, T., Rizzuto, R., Hajnoczky, G. & Su, T.P. *Trends Cell Biol.* **19**, 81–88 (2009).
- de Brito, O.M. & Scorrano, L. *Nature* **456**, 605–610 (2008).
- Csordas, G. et al. *J. Cell Biol.* **174**, 915–921 (2006).
- Varnai, P., Toth, B., Toth, D.J., Hunyady, L. & Balla, T. *J. Biol. Chem.* **282**, 29678–29690 (2007).



## ONLINE METHODS

**DNA construction.** Sequences encoding human FRB (T2098L) domain of mTOR and human FKBP12 were used for the generation of the following dimerization constructs.

For FRB-Giantin vector construction, a PCR product encoding Giantin (9391–9777) was digested using XhoI and BamHI, and then inserted into the multiple cloning site of the pEGFP-C1 (Clontech) vector in which *EGFP* was replaced with sequence encoding FRB.

For FRB-YFP-Giantin vector construction, Giantin vector (3131–3259) was digested using XhoI and BamHI from the FRB-Giantin vector, and then inserted into the multiple cloning site of the FRB-YFP vector<sup>2</sup>.

For FRB-MoA vector construction, a PCR product encoding Monoamine Oxidase A (490–527) was digested using EcoRI and BamHI, and then inserted into the multiple cloning site of the pEGFP-C1 vector in which *EGFP* was replaced with sequence encoding FRB.

For CFP-FKBP-Cb5 vector construction, a PCR product encoding cytochrome *b5* (100–134) was digested using EcoRI and BamHI, and then inserted into the multiple cloning site of the CFP-FKBP vector<sup>2</sup>.

For LAMP-FKBP vector construction, a PCR product encoding lysosomal-associated membrane protein 1 (1–417) was digested using EcoRI and BamHI, and then inserted into the artificially introduced digestion site of the pEGFP-C1 vector in which *EGFP* was replaced with sequence encoding FKBP.

For LAMP-CFP-FRB vector construction, a PCR product encoding lysosomal-associated membrane protein 1 (1–417) was digested using EcoRI and BamHI, and then inserted into the artificially introduced digestion site of the pEGFP-C1 vector in which *EGFP* was replaced with sequence encoding CFP-FRB.

For CFP-FKBP-RasGEF vector construction, a PCR product encoding the catalytic domain of RasGEF (RasGRF, 1003–1273) was digested using EcoRI and BamHI, and then inserted into the multiple cloning site of the pEGFP-C1 vector in which *EGFP* was replaced with sequence encoding CFP-FKBP<sup>16</sup>.

For Tom20-FRB vector construction, a PCR product encoding Tom20 (1–33) was digested using EcoRI and BamHI, and then inserted into the artificially introduced digestion site of the pEGFP-C1 vector in which *EGFP* was replaced with sequence encoding FRB.

For Tom20-CFP-FRB or Tom20-YFP-FRB vector construction, a PCR product encoding Tom20 (1–33) was digested using EcoRI and BamHI from Tom20-FRB, and then inserted into the artificially introduced digestion site of the pEGFP-C1 vector in which *EGFP* was replaced with sequence encoding CFP-FRB or YFP-FRB, respectively.

**Optimization of protein configuration.** The extent of translocation (the fraction of cytoplasmic fluorescence that translocated to each organelle) was different for each organelle (ER and mitochondria > lysosome > Golgi), primarily because of varying expression ratios between the anchor and effector units and/or to varying affinity between FKBP and FRB fusion proteins. In addition, the surface area of each organelle naturally limited the number of residential proteins. Thus, we changed constituents as well as the order of constituents in the chimeras, which are likely to affect protein stability and/or steric environment of the

FKBP-FRB interaction<sup>2</sup>. For instance, we swapped FKBP with FRB and also placed FKBP or FRB at N terminus or C terminus in relation to fluorescent proteins and targeting motifs.

**Transmission electron microscopy.** HeLa cells were transfected with vectors encoding Tom20-TFP-FRB and CFP-FKBP-Cb5 using EugeneHD (Roche). Eighteen hours after transfection, the cells in 100-mm-diameter dishes were treated with 5  $\mu$ M iRap for 15 min and then processed for transmission electron microscopy (TEM) as described previously<sup>16</sup>. Briefly, the cells were fixed for 1 h at room temperature (22–24 °C) in a solution containing 3% formaldehyde, 1.5% glutaraldehyde in 100 mM cacodylate containing 2.5% sucrose (pH 7.4). The cells were then lifted off the dish, pelleted and osmicated in Palade's OsO<sub>4</sub> (1 h at 4 °C). The pellet was then washed three times in 100 mM cacodylate (pH 7.4), treated with 1% tannic acid for 30 min at room temperature, washed three times in double-distilled water, and incubated overnight in Kellenberger's uranyl acetate. The pellet was then dehydrated through a graded series of ethanol washes and embedded in EMBED-812 Electron Microscopy Sciences. Sections were cut on a Leica Ultracut UCT ultramicrotome, collected onto 400-mesh nickel grids, stained with uranyl acetate and lead citrate, and observed in a Tecnai 12 at 100 kV. Images were collected with an Olympus SIS Megaview III charge-coupled device (CCD); and images were assembled in Adobe Photoshop with only linear adjustments in brightness and contrast.

**Quantification of TEM images.** Ten images that showed clear evidence of organelle tethering were selected. We made 200 linear measurements, with iTEM Olympus Soft Imaging Solutions analytical software, at discrete distances along the ER-outer mitochondrial membrane and calculated an average mean distance using Microsoft Excel.

**Cell culture and transfection.** Cell culture and transfection of HeLa and NIH3T3 cells were performed as described previously<sup>2</sup>.

**Live-cell confocal microscopy.** Live cell dual color measurements were performed on a spinning-disc confocal microscope. CFP and YFP excitations were conducted with helium-cadmium laser and argon laser (CVI-Melles Griot), respectively. The two lasers were fiber-coupled (OZ optics) to the spinning disk confocal unit (CSU10; Yokogawa) mounted with dual CFP/YFP dichroic mirrors (Semrock). The lasers were processed with appropriate filter sets for CFP and YFP (Chroma Technology) to capture fluorescence images with a CCD camera (Orca ER, Hamamatsu Photonics), driven by Metamorph 7.5 imaging software (Molecular Devices). Images were taken using a 40 $\times$  objective (Zeiss) mounted on an inverted Axiovert 200 microscope (Zeiss). Time-lapse live cell imaging using the confocal microscope was conducted as previously described<sup>2</sup>.

**Dimerization assays.** We used 5  $\mu$ M iRap to induce the dimerization events in all of the experiments described here. These events were also achieved by using 100 nM rapamycin. The cells were first transfected with an appropriate set of anchor and effector units. Twelve to twenty-four hours after transfection, we collected live-cell, time-lapse movies every 15 s for 10–15 min at room temperature using confocal microscopy. For colocalization assays, the

described anchor units were expressed along with the following organelle markers or co-stained with the small molecule dye. YFP-mito (the mitochondria targeting sequence from subunit VIII of cytochrome *c* oxidase, BD Biosciences Clontech), YFP-ER (the ER targeting sequence from calreticulin with the KDEL retrieval sequence, BD Biosciences Clontech), CFP-Golgi (the Golgi targeting sequence from 1,4-galactosyltransferase, BD Biosciences Clontech) and lysotracker (the small molecule lysosomal marker; Invitrogen).

**Western blot analysis.** HeLa cells, which we transfected with vectors encoding Tom20-YFP-FRB and CFP-FKBP-Cb5, or FRB-YFP-Giantin alone, were treated with dimerizers (5  $\mu$ M iRap or 100 nM rapamycin) and then were analyzed by western blot. We used anti-body to FRB (rabbit, Enzo Life Sciences ALX-215-065, lot L23209) and two antibodies to FKBP (both mouse; BD Biosciences 610909, lot 50423 or Affinity Bioreagent PA1-026A lot KH134289) for primary staining, together with two secondary antibodies labeled with fluorescent infrared dyes of different wavelengths (LI-COR Biosciences) that distinctively recognize rabbit or mouse IgG. Processed nitrocellulose membranes were imaged on an Odyssey Infrared Imaging System (LI-COR). For the quantification

of the proteins, Metamorph 7.5 imaging software (Molecular Devices) was used. Transfection efficiency for each condition was calculated based on the fluorescence images of the cells and taken into consideration for the final quantification.

**Visualization of fluorescently labeled phosphatidylserine.** Based on the previous report<sup>17</sup>, we used a fatty acid-labeled phosphatidylserine (1-palmitoyl-2-(12-((7-nitro-2-1,3-benzoxadiazol-4-yl)amino)lauroyl)-*sn*-glycero-3-phosphoserine or 16:0-12:0 NBD-PS from Avanti Polar Lipids). Before use, NBD-PS in chloroform was dried and then reconstituted in defatted BSA (Sigma) containing PBS with a rigorous vortex, which was then added to HeLa cells with an incubation of 30 min at 37 °C. After washing out an excess NBD-PS, the HeLa cells underwent live-cell time-lapse fluorescence imaging under the confocal microscope. A CFP channel was used to capture the NBD fluorescence signal.

**Statistical analyses.** Statistical analysis was performed using an unpaired *t*-test.

16. Perkins, E.M. & McCaffery, J.M. *Methods Mol. Biol.* **372**, 467–483 (2007).

17. Kobayashi, T. & Arakawa, Y. *J. Cell Biol.* **113**, 235–244 (1991).